NATIONAL ADVISORY COMMITTEE FOR AERONAUTICS

NACA

TECHNICAL NOTE 1967

A COMPARISON OF WING LOADS MEASURED IN FLIGHT ON A FIGHTER-TYPE AIRPLANE BY STRAIN-GAGE AND PRESSURE-DISTRIBUTION METHODS

By William S. Aiken, Jr., and Donald A. Howard

Langley Aeronautical Laboratory
Langley Air Force Base, Va.

Washington
November 1949

E R R A T A

NACA TN 1967

A COMPARISON OF WING LOADS MEASURED IN FLIGHT ON A FIGHTER-TYPE AIRPLANE BY STRAIN-GAGE AND PRESSURE-DISTRIBUTION METHODS

By William S. Aiken, Jr., and Donald A. Howard

November 1949

Page 6: Equation (5) should read $y_{cp} = \frac{C_{BM_A}}{C_{N_A}} \frac{b}{2}$

Page 6: Equation (6) should read $y_{cp} = 222.2 C_{BM_A}$

NACA-Langley - 3-8-50 - 1100

I

NATIONAL ADVISORY COMMITTEE FOR AERONAUTICS

TECHNICAL NOTE 1967

A COMPARISON OF WING LOADS MEASURED IN FLIGHT ON A FIGHTER-TYPE AIRPLANE BY STRAIN-GAGE AND PRESSURE-DISTRIBUTION METHODS

By William S. Aiken, Jr., and Donald A. Howard

SUMMARY

Pressure-distribution measurements were made on the wing of a fighter-type airplane to determine the span loading and to compare center-of-pressure results with those obtained by strain-gage measurements on the same airplane during a previous flight investigation. The flight tests were all made at a pressure altitude of about 30,000 feet and covered a Mach number range from approximately 0.35 to 0.81. Available wind-tunnel pressure-distribution data for a prototype of the test airplane are also included for comparison. Both flight and wind-tunnel pressure-distribution data are separated into additional and basic air load components.

The agreement between shears, bending moments, and spanwise centers of pressure determined in flight from pressure-distribution data and strain-gage data was found to be good. During buffeting in low-speed stalls the spanwise center of pressure shifted farther outboard than during buffeting at Mach numbers near 0.80.

INTRODUCTION

Strain-gage installations are being used extensively to measure the loads on component parts of airplanes in flight. Although flight-test results indicate that such installations are satisfactory, few, if any, direct checks made against pressure-distribution measurements exist.

A fighter-type airplane which was being used in a buffeting investigation was equipped with pressure-recording equipment, and a limited number of flights were made to check the results of strain-gage measurements of wing loads as previously reported in reference 1. The tests were made at a pressure altitude of about 30,000 feet and covered a Mach number range from approximately 0.35 to 0.81.

The analysis of the span-loading data obtained in flight was not confined only to comparing spanwise center-of-pressure data from the pressure-distribution measurements with the strain-gage results of reference 1 but was extended to include a separation of the air load into additional and basic distributions. Since wind-tunnel span loadings for a prototype of the test airplane were available, these data were also analyzed on the same basis and compared with the flight pressure-distribution data. Some of the tests extended to buffeting conditions; therefore, span loadings obtained during buffeting are presented and discussed since there is a scarcity of data in this region.

SYMBOLS

c_n	section normal-force coefficient $\left(\int_0^1 \frac{\Delta p}{q} d\frac{x}{c}\right)$
Δp	differential pressure (lower surface minus upper surface)
q	dynamic pressure
$\frac{x}{c}$	fraction of wing chord
C_N	wing normal-force coefficient outboard of reference station, in terms of complete wing area
y	distance along semispan from airplane center line
$\frac{b}{2}$	wing semispan
c	wing chord
$\bar{c}$	mean geometric chord of complete wing
M	Mach number
n	airplane normal acceleration at center of gravity, measured perpendicular to thrust line, g units
g	acceleration due to gravity
c_{n_a}	section normal-force coefficient due to additional air load
c_{n_b}	section normal-force coefficient due to basic load distribution

C_{BM} bending-moment coefficient outboard of reference station in terms of complete wing area

y_{cp} spanwise distance of center of pressure of air load on wing from reference station, inches

Subscripts:

A total additional air load

B total basic load

APPARATUS AND TESTS

Airplane

The airplane used in the investigation was the same airplane used in the investigations reported in references 1 and 2. The horizontal tail, fuselage, wing, canopy, and cowling had been heavily reinforced to provide an extra safety margin against structural failure in an investigation of buffeting loads. Pertinent geometric characteristics of the airplane are given in the three-view diagram of figure 1 and in the following table:

Wing:	
Span, feet	37.03
Area, square feet	240.1
Mean aerodynamic chord, feet	6.63
Airfoil	Low drag
Aspect ratio	5.7
Weight during tests, pounds	8750
Center-of-gravity position during tests, percent M.A.C.	25.1

Instrumentation

Standard NACA recording instruments were used to record time histories of impact pressure, pressure altitude, normal center-of-gravity acceleration, right and left aileron position, elevator position, rate of pitch, and elevator and aileron stick forces. A timer was used to correlate data from all recording instruments.

The airspeed head was mounted on a boom extending 1.2 local chords ahead of the right wing tip. The airspeed-altitude recorder was located in the right wing ammunition compartment in order to reduce the tubing length and therefore minimize any lag effects. The entire airspeed system was calibrated by radar tracking for position error up to a Mach number of 0.78.

The pressure-distribution measuring system consisted of two recording manometers which were connected by means of aluminum tubing to orifices installed in the left and right wings. The spanwise location of the orifice rows used with relation to the wing plan form is shown in figure 1. Three rows located at semispan stations $\frac{y}{b/2} = 0.211$, 0.513, and 0.833 were used on the left wing and two rows located at semispan stations $\frac{y}{b/2} = 0.211$ and 0.513 were used on the right wing. The chordwise locations of the orifices on the upper and lower surfaces of the left wing are given in table I. Since the upper- and lower-surface orifices were connected to measure differential pressures, the average location in percent of chord as given in table I was used in evaluating section data.

Tests

The flight pressure-distribution data were all obtained at a pressure altitude of about 30,000 feet. Pull-up maneuvers were made at Mach numbers of 0.355, 0.404, 0.496, 0.580, 0.681, 0.761, 0.770, and 0.807. In all cases below the stall the Mach number was constant within an average of $\pm\frac{1}{2}$ percent. The pull-up at a Mach number of 0.355 was continued until the airplane stalled and the pull-ups at Mach numbers of 0.770 and 0.807 were continued until a condition of buffeting existed.

All flights were made with power on and with the airplane in the clean condition. Before each maneuver, stick forces were trimmed in level flight and the pull-up was made with no intentional aileron deflection or sideslip.

METHOD OF ANALYSIS

The method outlined in the following paragraphs was used to reduce both flight and wind-tunnel span load distributions to additional and basic air load distributions. The additional air load distribution is the load distribution dependent only on angle of attack or normal-force

coefficient for a given value of Mach number and pressure altitude. The basic air load distribution is a load distribution independent of angle of attack and varying with Mach number and dynamic pressure. This type of load distribution by definition has zero total lift.

Typical flight span loadings for $M = 0.496$ and $M = 0.770$ are shown in figure 2 where the load coefficient $c_n\frac{c}{\bar{c}}$ is plotted against semispan position. Since the strain gages were located at the semispan station $\frac{y}{b/2} = 0.1575$, the fairing of the load-distribution curves extended to this station. The first step in reducing the data was to integrate each span loading to obtain the normal-force coefficient outboard of station 0.1575. This quantity is defined as

$$C_N = \int_1^{0.1575} c_n\frac{c}{\bar{c}}\, d\left(\frac{y}{b/2}\right) \tag{1}$$

The integrated values of C_N for typical pull-up maneuvers are given in figure 2.

The next step in the procedure is illustrated in figure 3 where the values of the section load coefficient $c_n\frac{c}{\bar{c}}$ measured at each of the three spanwise stations are plotted against C_N. The variations of $c_n\frac{c}{\bar{c}}$ with C_N are noted to be reasonably close to a straight line so that, for constant altitude and constant Mach number conditions, the distribution of load over the wing semispan may be separated into an additional air load component $c_{n_a}\frac{c}{\bar{c}}$ and a basic air load component $c_{n_b}\frac{c}{\bar{c}}$. The section load coefficient at any point along the span may be expressed as

$$c_n\frac{c}{\bar{c}} = c_{n_a}\frac{c}{\bar{c}} + c_{n_b}\frac{c}{\bar{c}} \tag{2}$$

By definition the section additional-air-load coefficient changes with total load; whereas the section basic-air-load coefficient has a constant value which corresponds to zero total load over the portion of the span considered. Equation (2) may therefore be rewritten as follows:

$$c_n\frac{c}{\bar{c}} = \frac{dc_{n_a}\frac{c}{\bar{c}}}{dC_N} C_N + c_{n_b}\frac{c}{\bar{c}} \tag{3}$$

The slopes of the curves of figure 3 $\frac{dc_{n_a}\frac{c}{\bar{c}}}{dC_N}$ represent the section additional-air-load coefficients; whereas the zero intercepts correspond to the basic load coefficients. Both slopes and intercepts were determined by the method of least squares. The slope corresponds to a value of $C_N = 1.0$ with the assumption that the relationship remains linear up to $C_N = 1.0$.

As an aid in the determination of the additional and basic load distributions, slopes and intercepts were evaluated from the faired span loadings at spanwise stations other than 0.211, 0.513, and 0.833. All additional and basic load distributions were determined in the manner described.

The center of pressure of the additional air load for the pressure-distribution results was determined from the bending-moment coefficient which is defined as follows:

$$C_{BM_A} = \int_1^{0.1575} \int_1^{0.1575} \frac{dc_{n_a}\frac{c}{\bar{c}}}{dC_N} d\left(\frac{y}{b/2}\right) d\left(\frac{y}{b/2}\right) \tag{4}$$

and the equation

$$y_{cp} = \frac{C_{BM_A}}{C_{N_A}}(1 - 0.1575)\frac{b}{2} \tag{5}$$

Since $C_{N_A} = 1.0$ and $\frac{b}{2} = 222.2$, equation (5) reduces to

$$y_{cp} = 187.2C_{BM_A} \tag{6}$$

The bending-moment coefficient for the basic load was obtained from the equation

$$C_{BM_B} = \int_1^{0.1575} \int_1^{0.1575} c_{n_b}\frac{c}{\bar{c}} d\left(\frac{y}{b/2}\right) d\left(\frac{y}{b/2}\right) \tag{7}$$

RESULTS AND DISCUSSION

Direct comparison of pressure-distribution measurements of wing shear and wing bending moment with strain-gage results obtained during the tests reported in reference 1 was practical in only two cases. In figure 4 the variation of aerodynamic shear outboard of station 0.1575 is shown as a function of airplane normal acceleration. The flight-test strain-gage data are for an average Mach number of 0.777 at a pressure altitude of 30,000 feet; the flight-test pressure-distribution data are for an average Mach number of 0.771 at the same altitude. The agreement is considered excellent. In figure 5 the variation of wing aerodynamic bending moment outboard of station 0.1575 is shown as a function of airplane normal acceleration. The strain-gage and pressure-distribution data are for the same conditions as listed in figure 4. The agreement for this case is not so good as that of figure 4; however, both strain-gage data and pressure-distribution data have approximately the same slope per g. The difference between the pressure-distribution data and the strain-gage data may be due to either strain-gage zero shifts or to the fairing of the span loadings near the tip.

Consideration of figures 4 and 5 together shows that the strain-gage results are just as consistent as the pressure-distribution results and that determining which method of measurement gives the best accuracy would be only a matter of opinion.

Additional air load.- Figure 6 is a plot of the left-wing spanwise additional load distributions outboard of station 0.1575 for the Mach numbers covered in the present series of flight tests. Load coefficient is plotted against semispan station and for purposes of comparison each distribution is based on a value of $C_N = 1.0$. In all cases except that for $M = 0.807$ the additional air load applies to unstalled conditions or to airplane lift coefficients below the buffeting boundary. The distributions are noted to be quite similar with the exception of those at Mach numbers of 0.807 and 0.761. The deviation of the curve for a Mach number of 0.761 from the general shape shown by the other curves is difficult to understand since it applies below the buffeting and stall boundaries. Limited data obtained on the right wing at $M = 0.761$ showed the same trend, that of decreased loading near the root and increased loading over the midsemispan section.

The additional-air-load curve for a Mach number of 0.807 shows a definite change in shape with an increase in loading near the wing tip. This curve was derived from limited data at airplane normal-force coefficients above the high-speed buffeting boundary. The shape of this curve may be due to the partial stall existing on the wing, to Mach number effects, or to inadequate data.

In figure 7 are shown additional air load distributions derived in the same manner from Ames 16-foot high-speed tunnel data for a $\frac{1}{3}$-scale model of a prototype of the test airplane. The C_N values for all curves are equal to 1.0. These curves represent approximately the same Mach number range as shown in figure 6. An increasing outboard shift of the load may be observed as the Mach number increases from 0.398 to 0.797 which does not agree with the flight data in figure 6. Before a direct comparison of the two sets of data can be made, the torsional rigidity and elastic axis location of both wing structures would have to be known. The outboard shift of the additional air load shown in figure 7 is characteristic of the aeroelastic effect when the elastic axis is behind the aerodynamic center.

There are other possible reasons for the discrepancies which exist between the wind-tunnel and flight span loading data. Among these reasons are (1) the wind-tunnel section data are not corrected to free-air conditions and (2) the wind-tunnel and flight tests were made at different effective altitudes. With regard to the second point, if the flight tests had been made at altitudes other than 30,000 feet, different span loadings would result.

Spanwise center of pressure of additional air load.- The variation with Mach number of the additional-air-load center of pressure outboard of station $\frac{y}{b/2} = 0.1575$ is given in figure 8 for the pressure-distribution and strain-gage measurements. With the exception of the point at a Mach number of 0.807, the flight-pressure-distribution centers of pressure fall within the scatter of the strain-gage results. Two possible reasons may account for the tendency of the pressure-distribution center of pressure to be farther outboard on the average than the strain-gage results; namely, (1) the fairing of the span loading curves near the tip may have introduced discrepancies and (2) inertia load corrections to the strain-gage data may not have been exact because of the difficulty of determining the actual wing weight distribution. In general the agreement between the flight strain-gage and pressure-distribution measurements is considered excellent.

In figure 9 the flight-test pressure-distribution centers of pressure outboard of station $\frac{y}{b/2} = 0.1575$ are compared with Ames 16-foot high-speed tunnel results scaled to full airplane size for various Mach numbers. General agreement may be noted with more scatter in the flight-test values than the wind-tunnel results. The wind-tunnel results show a consistent outboard movement of the additional air-load center of pressure with increasing Mach number which is not evidenced by flight-test strain-gage or pressure-distribution data.

Basic air load distribution.- The basic air load distributions derived from flight-test data are given in figure 10 as a function of semispan station for the Mach numbers of the tests. Bending-moment coefficients C_{BM_B} are listed for each distribution as a guide in estimating the effect of Mach number. The C_{BM_B} variation and the shape of the curves show no consistent trend with Mach number, which may be due to the fact that the aileron angles were not exactly the same for all tests.

In figure 11 the spanwise basic air load distribution is shown as derived from wind-tunnel data for the same Mach numbers as given for the additional distributions in figure 7. Since the geometric twist at the wing tip and zero lift pitching-moment coefficient are both negative, an increase of the C_{BM_B} of the basic load distribution would be expected for increasing Mach numbers. In comparisor with the flight data, the wind-tunnel tests show a more consistent outboard load shift with a corresponding increase in C_{BM_B} occurring as the Mach number increases from 0.398 to 0.797.

Span loading during a stall and buffeting.- In the series of flight-test maneuvers reported herein, one pull-up was made to a stalled condition at a low Mach number (approximately 0.35) and several pull-ups were made past the buffeting boundary at Mach numbers of approximately 0.76, 0.77, and 0.81. Although these tests were not extensive enough to indicate specific trends, the results indicate in a general way the differences existing between unstalled spanwise load distributions, stalled conditions at low Mach numbers, and buffeting at Mach numbers near 0.8.

Time histories of pressure altitude, Mach number, and normal acceleration are shown in figure 12 for a pull-up to a stall at a Mach number of approximately 0.35. Figure 13 gives the spanwise load distribution for the left wing corresponding to the maneuver of figure 12. Load coefficient is plotted against semispan station for selected times during the maneuver. At 0.1 second the airplane is not stalled and the load distribution is normal with the center of pressure about 75 inches outboard of $\frac{y}{b/2} = 0.1575$. At 0.3 second the airplane has begun to stall as shown by the oscillations on the normal-acceleration time history (fig. 12) and the load has shifted slightly outboard with the center of pressure at approximately 79 inches. The integrated normal-force coefficient of the wing has reached its maximum value at a time of 0.3 second. At 0.6 second the stall is complete and the center of pressure has shifted outboard to approximately 85 inches. The value of C_N has begun to fall off and continues to do so for the remaining

span loadings shown in figure 13. As the time progresses from 0.6 to 1.0 second, the center of pressure of the wing moves gradually inboard as the wing begins to return to the unstalled condition. An interesting comparison can be made for the span loadings at 0.1 and 1.0 second since both have the same wing C_N values and approximately the same Mach number. The center of pressure for 0.1 second, at which time an unstalled condition exists, is at 74.9 inches; whereas the center of pressure for 1.0 second, at which time a stalled condition exists, is at 82.4 inches. In other words the aerodynamic bending moment for the particular stalled condition considered is 10 percent greater near the wing root than for the unstalled case.

Time histories of pressure altitude, Mach number, and normal acceleration are illustrated in figure 14 for a pull-up into the high-speed buffeting region. The Mach number is roughly constant and the altitude change is less than 1000 feet. The normal-acceleration time history shows a slight vibration of the airplane to exist from a time of -0.40 to about 0.35 second. Buffeting is not considered to begin until a time of 0.35 second is reached; then the average normal acceleration is about 2.5g. In figure 15 the span loadings corresponding to various times during the maneuver of figure 14 are illustrated. For the first three times illustrated, buffeting of appreciable magnitude has not begun and the span loadings are quite normal. The center of pressure moves inboard again as the normal-force coefficient decreases.

Although the derived additional air load distribution during buffeting at a Mach number of 0.807 (illustrated in fig. 6) indicated an outboard shift in load, the validity of this span loading is doubtful because of the difficulty in evaluating the pressure records during severe buffeting. The total span loadings for $M = 0.807$ differ very little in shape from those shown for $M = 0.770$ in figure 15.

In general it appears that within the limits of these flight tests, high-speed buffeting conditions do not seriously affect the span loadings. During buffeting that occurs when a complete stall is reached, however, the center of pressure shifts outboard as much as 10 inches for comparable wing-load values.

CONCLUSIONS

From the comparisons of the flight pressure-distribution measurements with strain-gage measurements and wind-tunnel tests of a prototype of the test airplane, the following conclusions were drawn:

1. The agreement between flight pressure-distribution measurements of wing root shear and bending-moment and flight strain-gage measurements of the same quantities was good for the limited cases where comparison was possible.

2. The agreement shown between flight pressure-distribution measurements and flight strain-gage measurements of the additional-air-load spanwise center of pressure was good.

3. The consistent outboard movement with increasing Mach number of the wind-tunnel spanwise additional-air-load center of pressure was not evidenced by the flight strain-gage or pressure-distribution data.

4. The outboard load shift with increasing Mach number of the wind-tunnel basic air load distributions was more consistent than the flight pressure-distribution results.

5. Buffeting had no serious effect on span loading for the conditions investigated.

6. The spanwise center of pressure shifted farther outboard during low-speed stalls than during buffeting at Mach numbers near 0.8.

Langley Aeronautical Laboratory
National Advisory Committee for Aeronautics
Langley Air Force Base, Va., August 1, 1949

REFERENCES

1. Aiken, William S., Jr.: Flight Determination of Wing and Tail Loads on a Fighter-Type Airplane by Means of Strain-Gage Measurements. NACA TN 1729, 1948.

2. Stokke, Allen R., and Aiken, William S., Jr.: Flight Measurements of Buffeting-Tail Loads. NACA TN 1719, 1948.

TABLE I

LEFT-WING PRESSURE-ORIFICE LOCATIONS

[All values are in percent of chord]

	Station 48 $\left(\frac{y}{b/2} = 0.211\right)$			Station 114 $\left(\frac{y}{b/2} = 0.513\right)$			Station 185 $\left(\frac{y}{b/2} = 0.833\right)$		
Orifice	Upper surface	Lower surface	Average	Upper surface	Lower surface	Average	Upper surface	Lower surface	Average
1	0.50	0.52	0.51	0.64	0.52	0.58	0.68	0.57	0.62
2	2.33	2.32	2.32	2.54	2.59	2.56	2.36	2.41	2.38
3	5.40	5.69	5.54	5.52	5.58	5.55	5.41	5.47	5.44
4	9.27	9.27	9.27	9.64	9.55	9.59	9.51	9.46	9.48
5	14.50	14.67	14.58	14.79	14.67	14.73	14.46	14.49	14.48
6	20.43	20.05	20.24	21.30	21.30	21.30	20.55	20.35	20.45
7	26.88	26.57	26.72	26.26	26.23	26.24	27.26	27.20	27.23
8	35.17	34.68	34.92	35.24	35.30	35.27	34.17	34.18	34.17
9	40.46	40.32	40.39	42.28	42.16	42.22	44.00	43.95	43.97
10	48.19	48.10	48.14	50.03	50.07	50.05	49.00	49.14	49.07
11	58.63	58.77	58.70	57.12	57.03	57.07	59.07	58.95	59.01
12	65.27	65.12	65.19	66.29	66.34	66.31	65.51	65.20	65.35
13	75.04	74.99	75.01	72.80	72.75	72.78	72.63	72.51	72.57
14	80.05	79.88	79.96	79.38	79.19	79.28	78.81	78.71	78.76
15	85.45	85.26	85.35	84.59	84.57	84.58	85.19	85.04	85.11
16	90.44	90.27	90.35	90.38	90.31	90.34	90.40	90.02	90.21
17	94.08	93.97	94.02	94.64	94.58	94.61	93.82	93.82	93.82
18	97.47	97.66	97.56	97.23	97.19	97.21	96.99	96.99	96.99

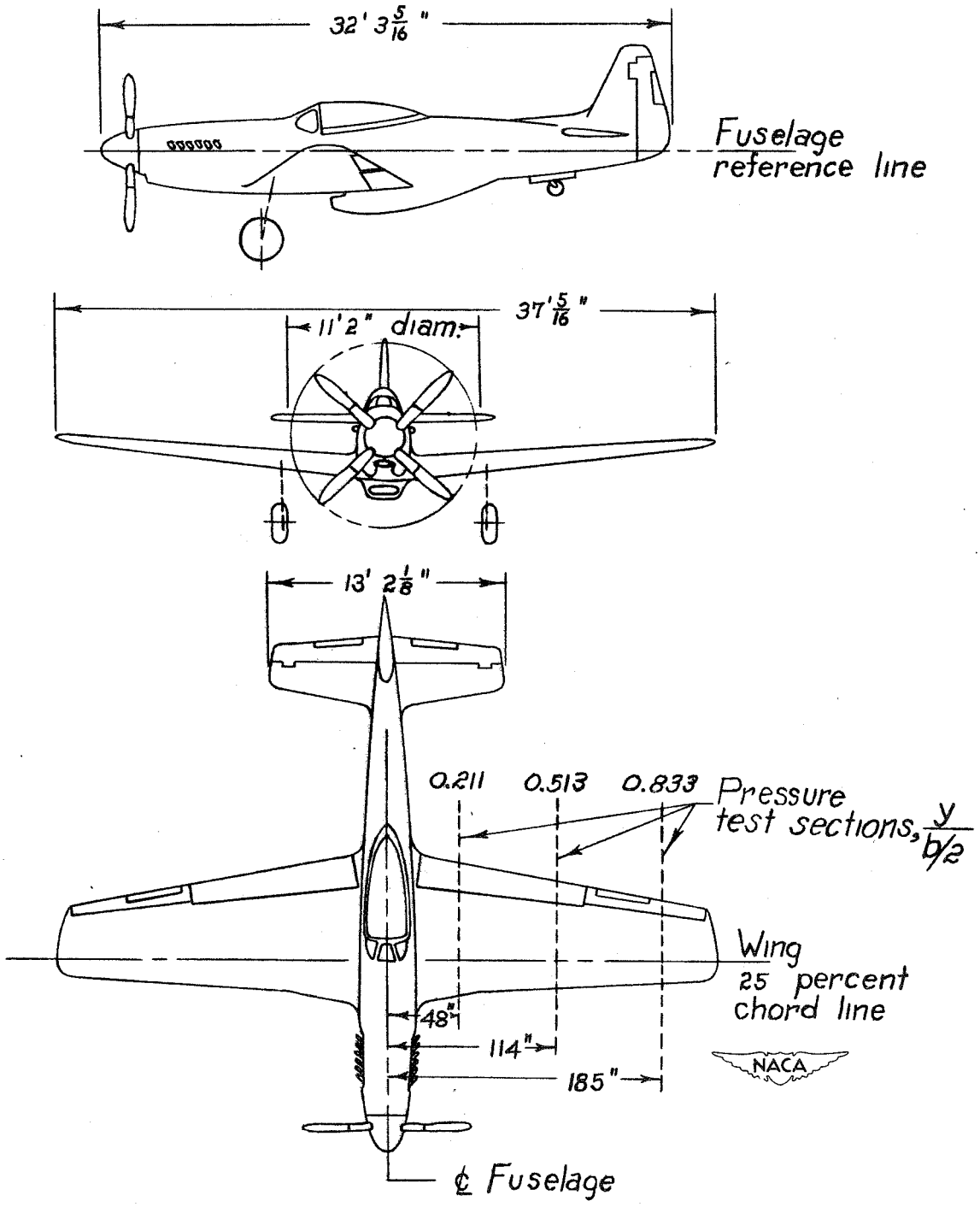

Figure 1.- Three-view diagram of test airplane.

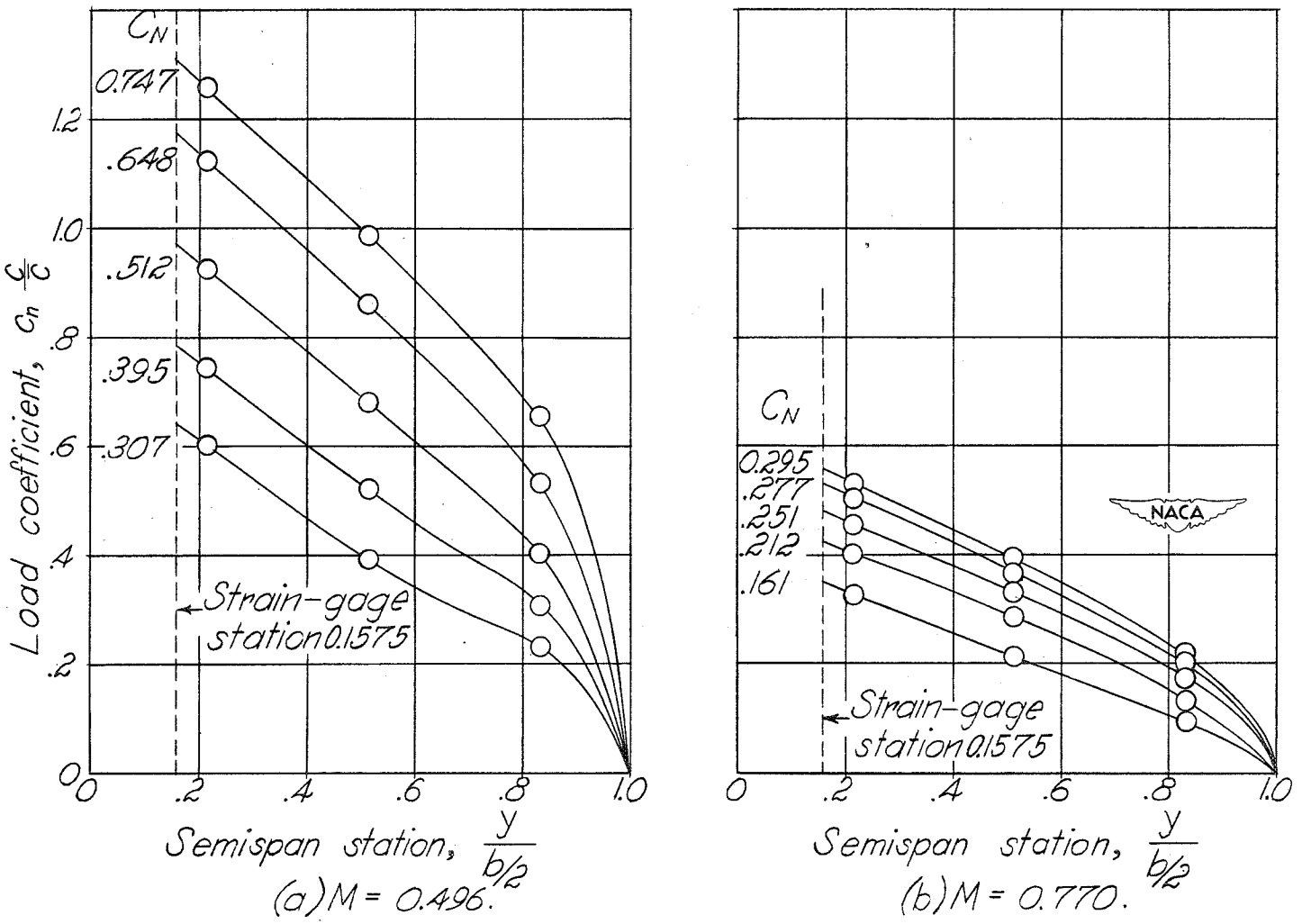

Figure 2.– Typical spanwise load distributions obtained in flight at several values of wing normal-force coefficient for two Mach numbers.

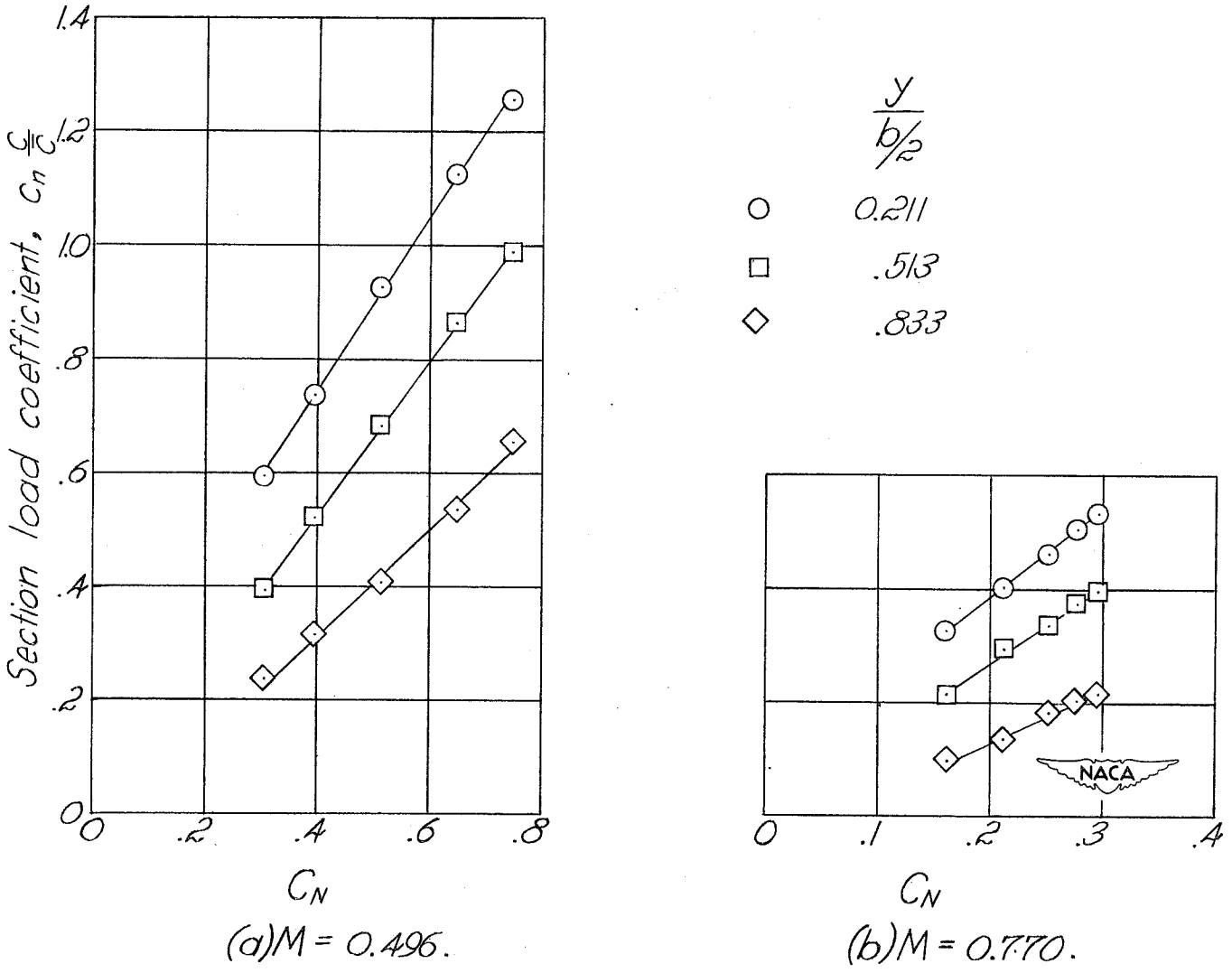

Figure 3.– Typical section load coefficient variations at two Mach numbers.

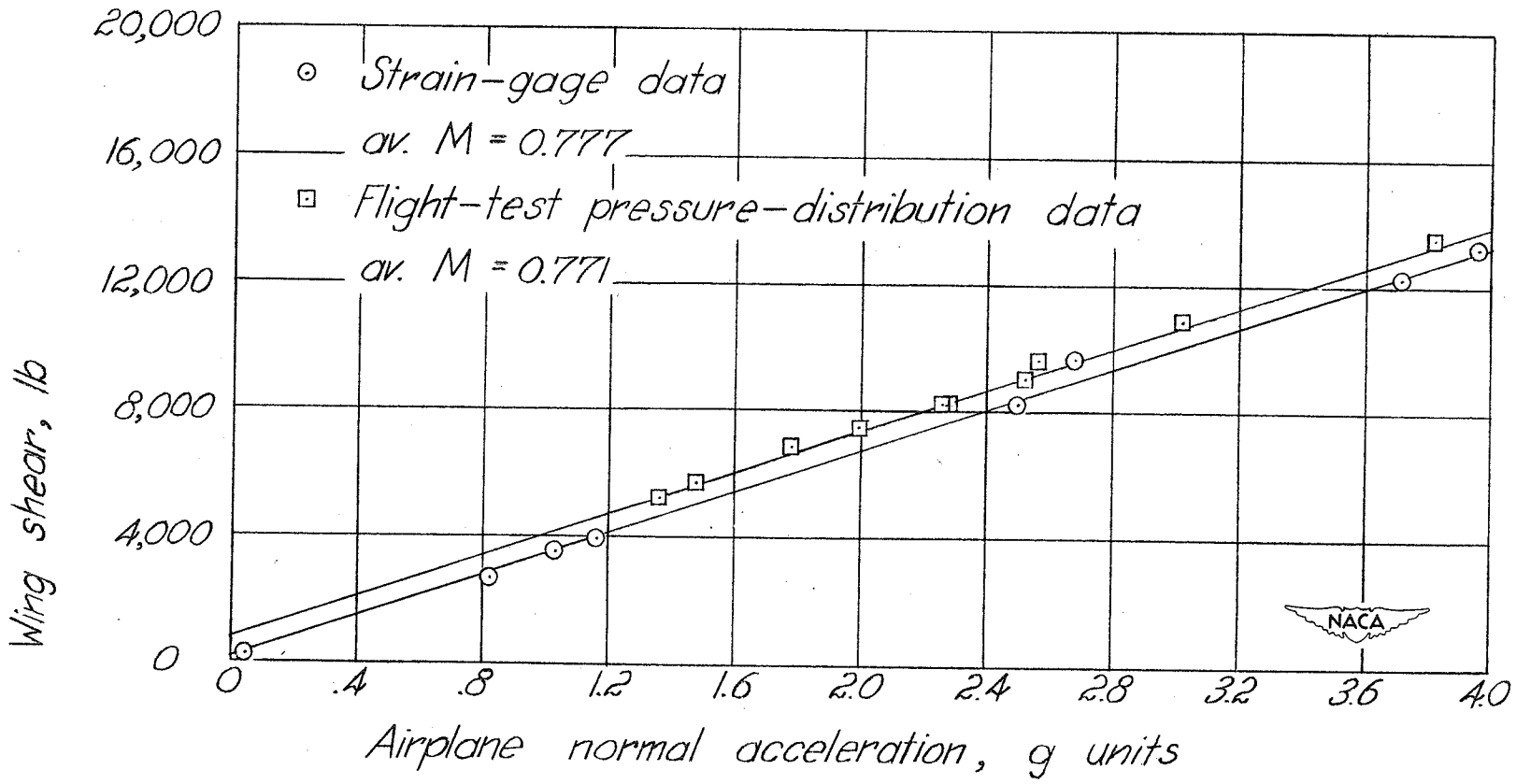

Figure 4.– Comparison of flight strain-gage and pressure-distribution measurements of wing shear outboard of station $\frac{y}{b/2} = 0.1575$ for test airplane.

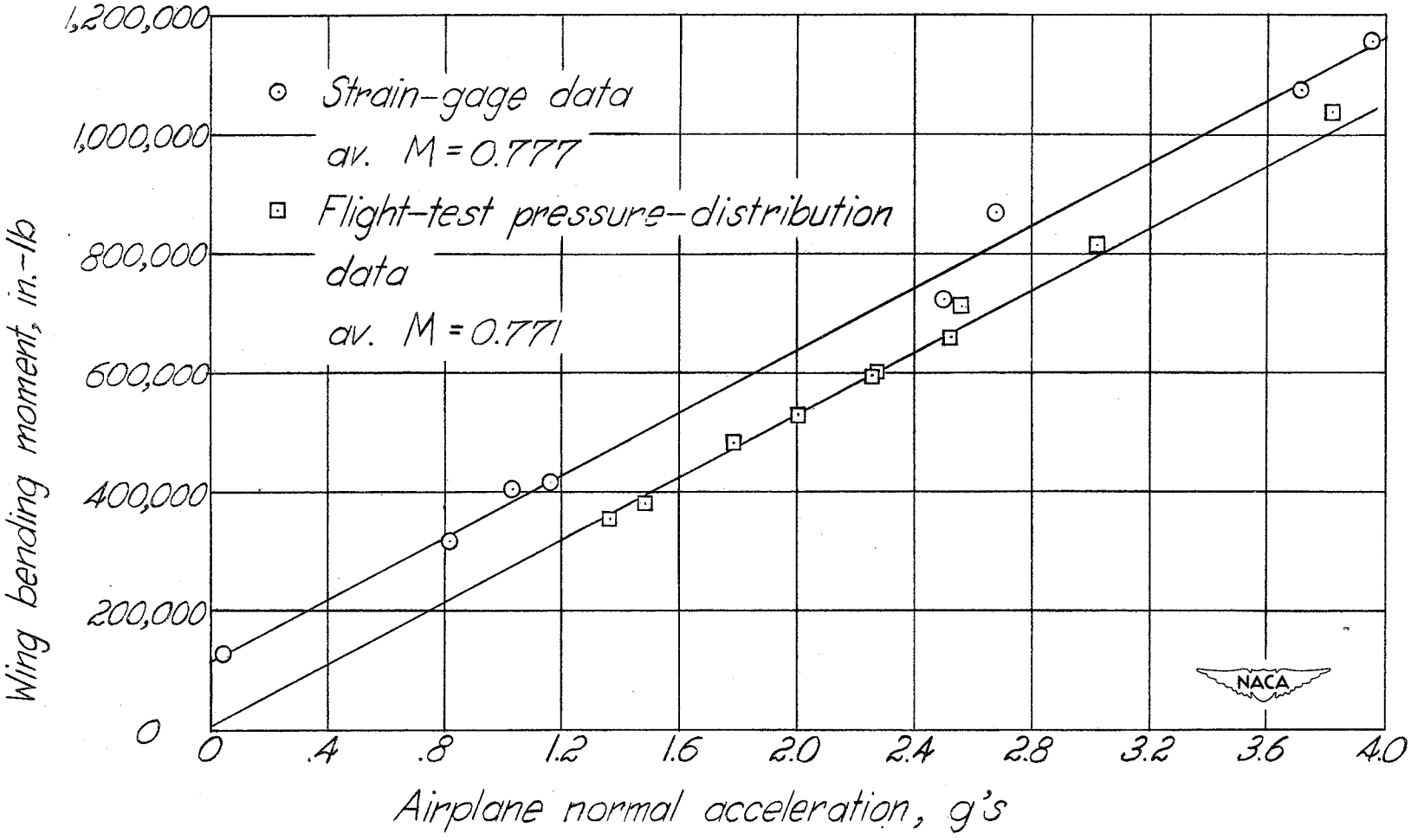

Figure 5.– Comparison of flight strain-gage and pressure-distribution measurements of wing aerodynamic bending moment outboard of station $\frac{y}{b/2} = 0.1575$ for test airplane.

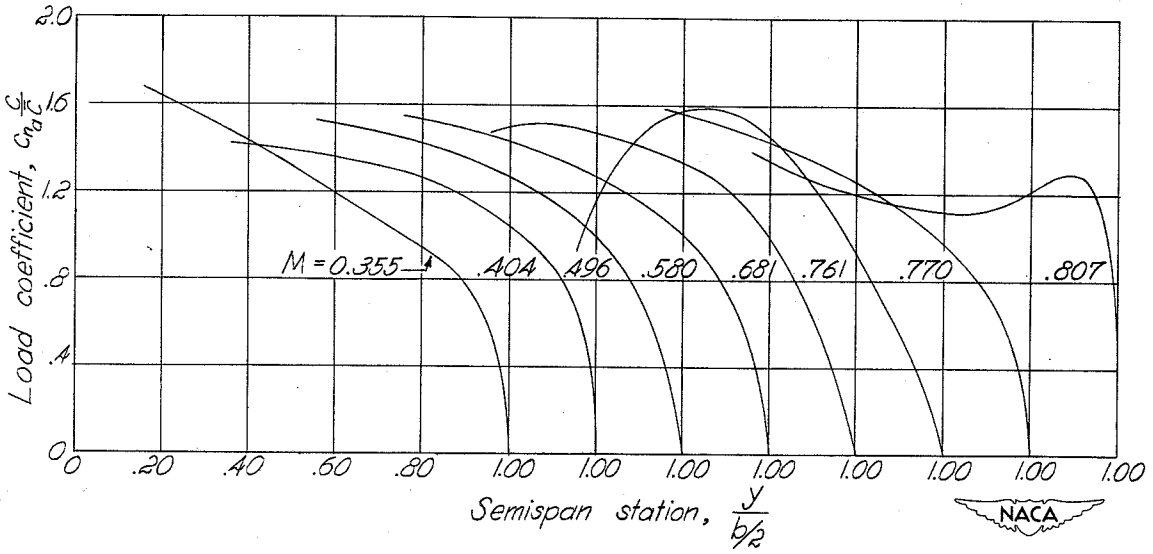

Figure 6.– Left–wing spanwise distributions of additional air load (C_N = 1.0) throughout the Mach number range covered in flight tests.

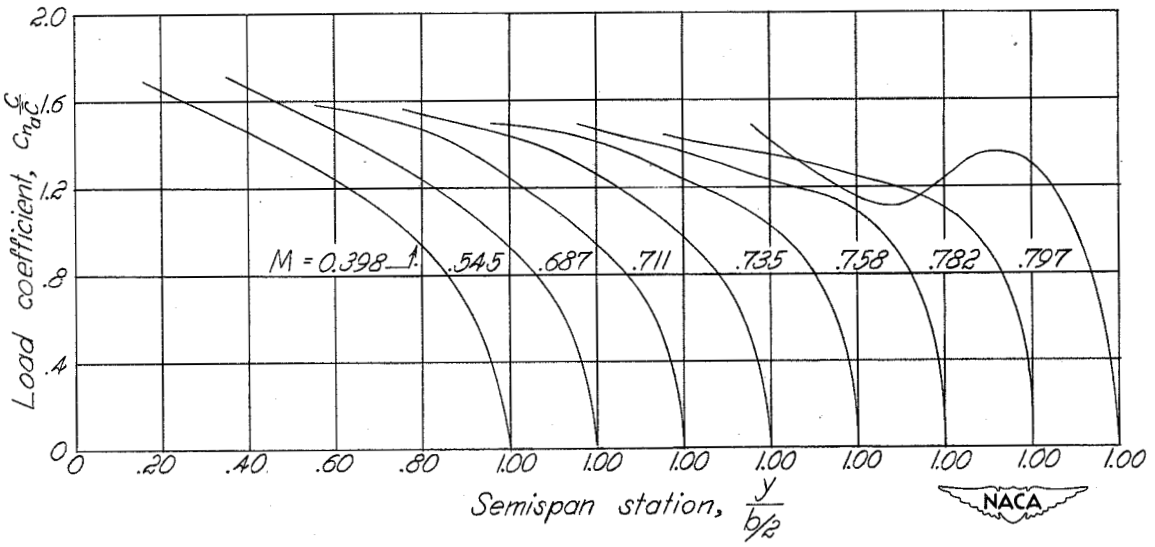

Figure 7.– Spanwise distributions of additional air load (C_N = 1.0) for several values of Mach number as derived from Ames 16–foot high–speed wind–tunnel data on a $\frac{1}{3}$–scale model of a prototype of the test airplane.

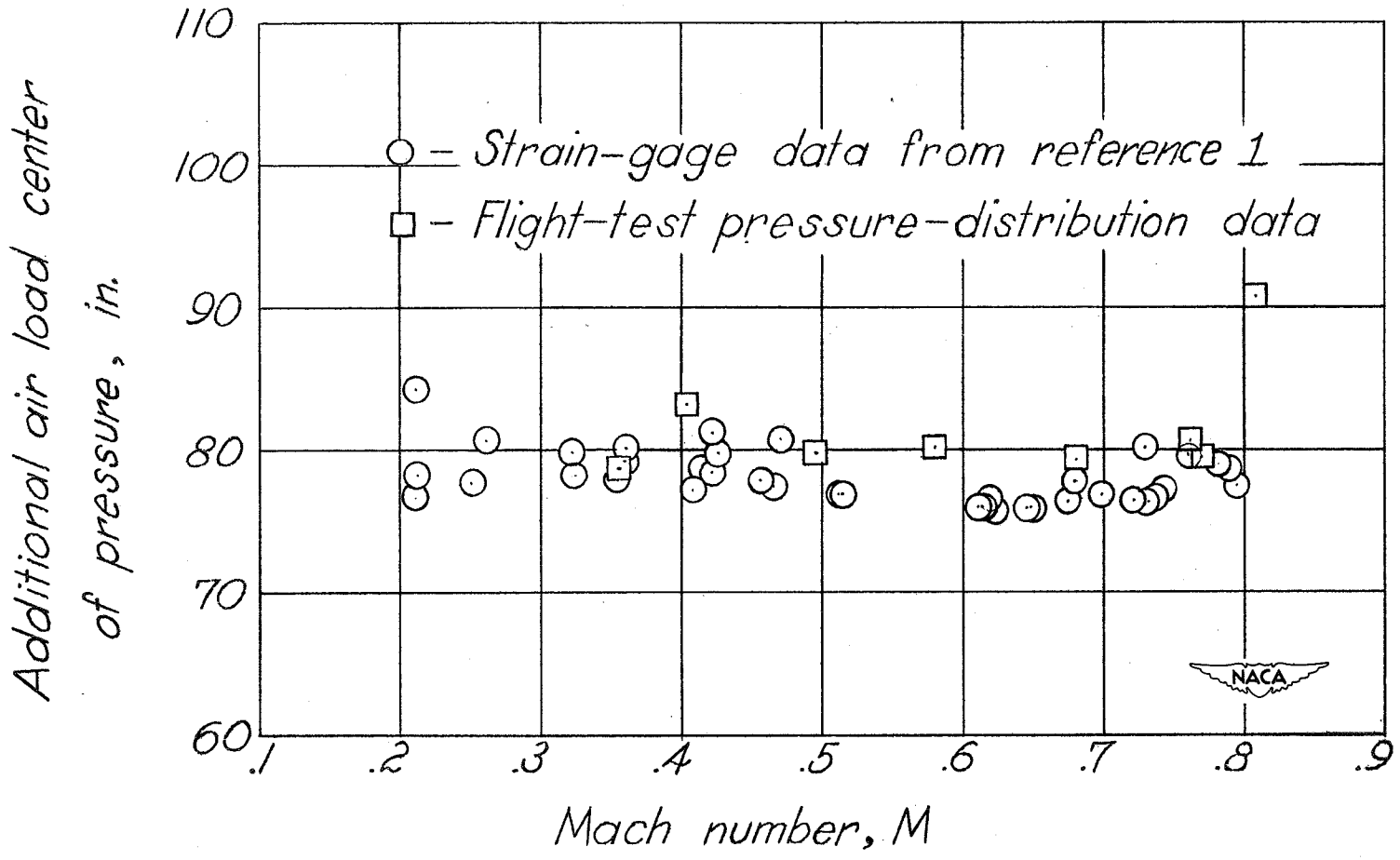

Figure 8.- Flight-test pressure-distribution and strain-gage additional-air-load centers of pressure outboard of station $\frac{y}{b/2} = 0.1575$.

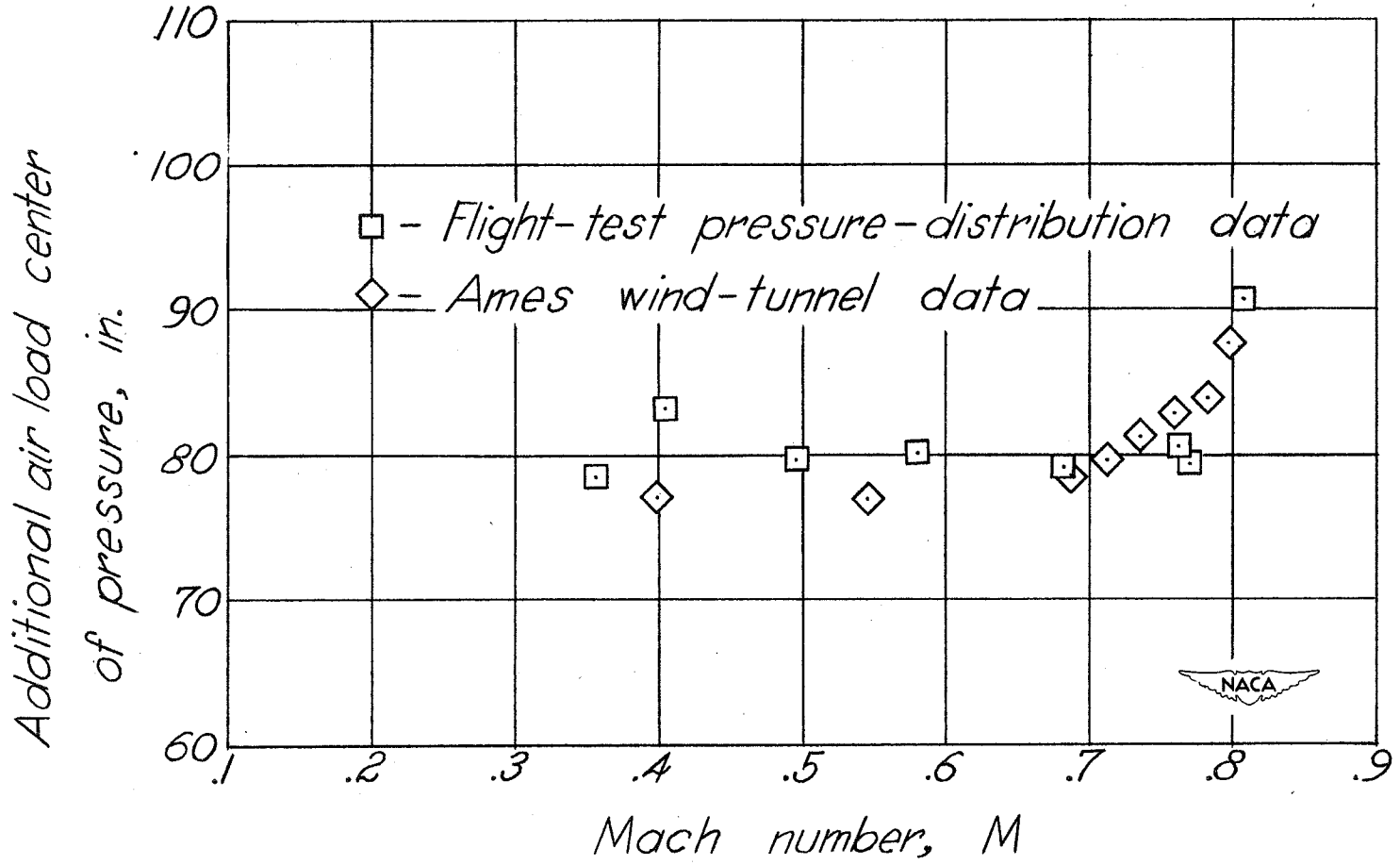

Figure 9.- Flight-test pressure-distribution and Ames 16-foot high-speed wind-tunnel additional-air-load centers of pressure outboard of station $\frac{y}{b/2}$ of 0.1575. Wind-tunnel data scaled to airplane size.

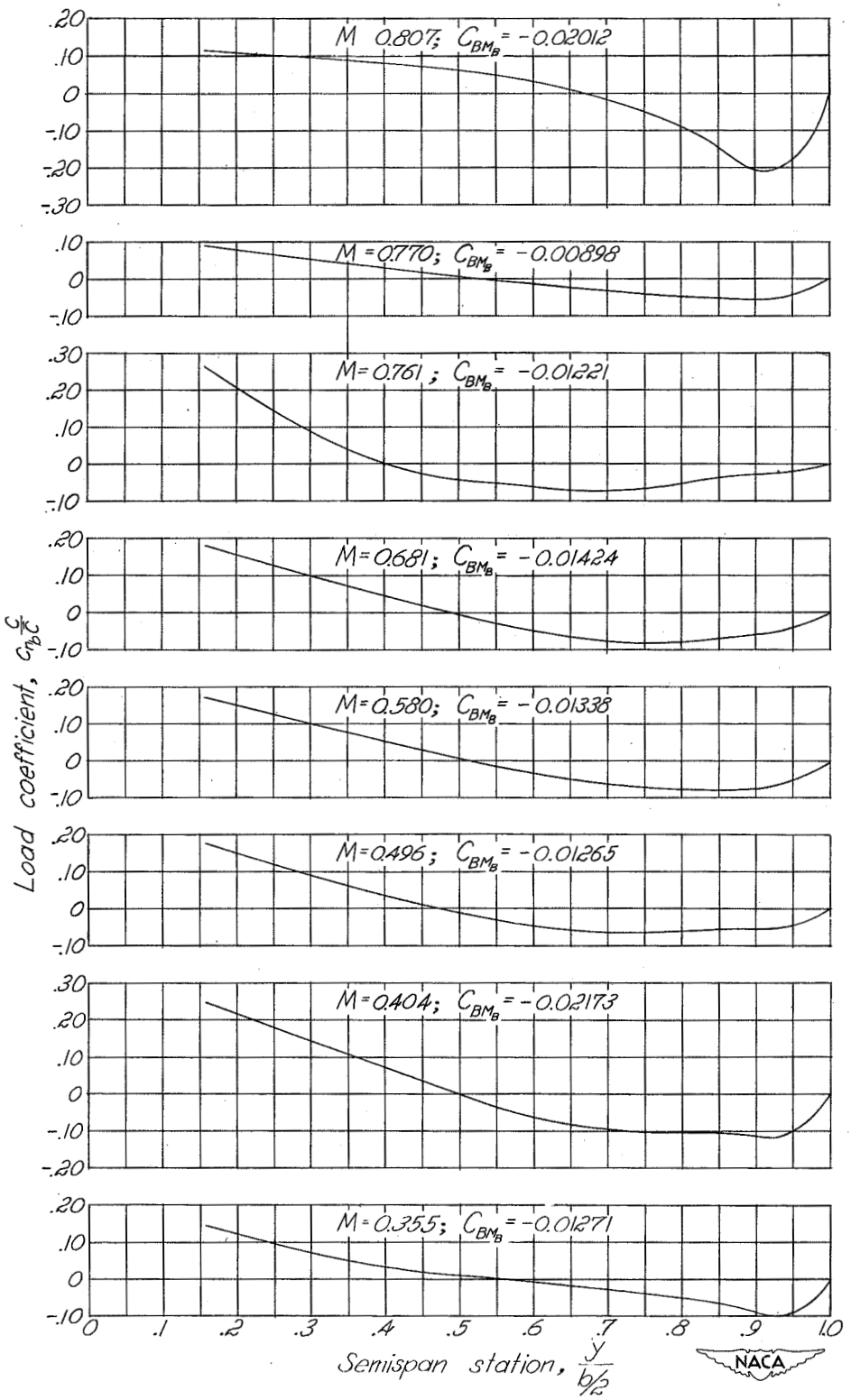

Figure 10.- Spanwise distribution of basic air load throughout the Mach number range covered in flight tests.

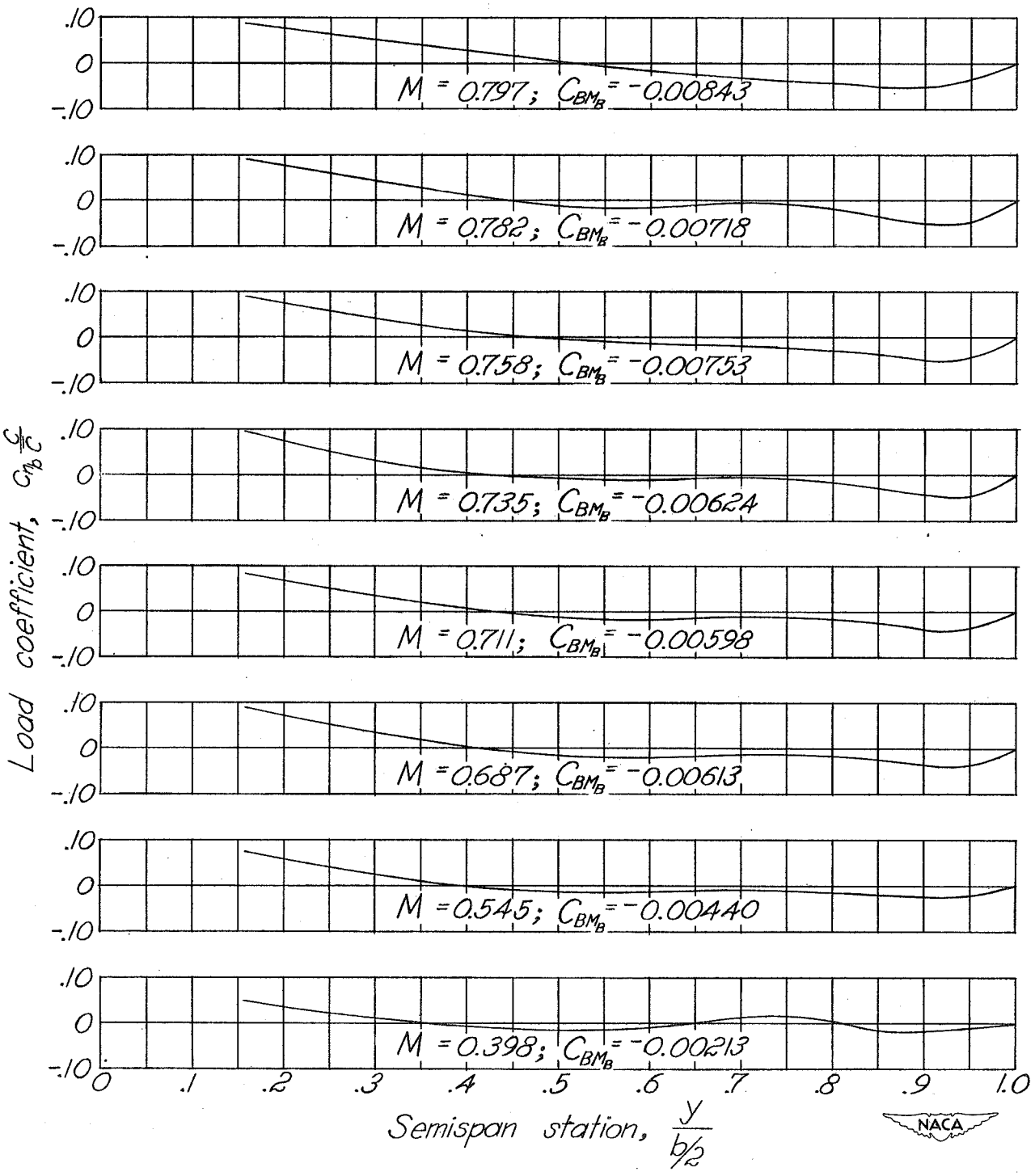

Figure 11.— Spanwise distribution of basic air load throughout the Mach number range covered in Ames 16-foot high-speed wind-tunnel tests on a $\frac{1}{3}$-scale model of a prototype of the test airplane.

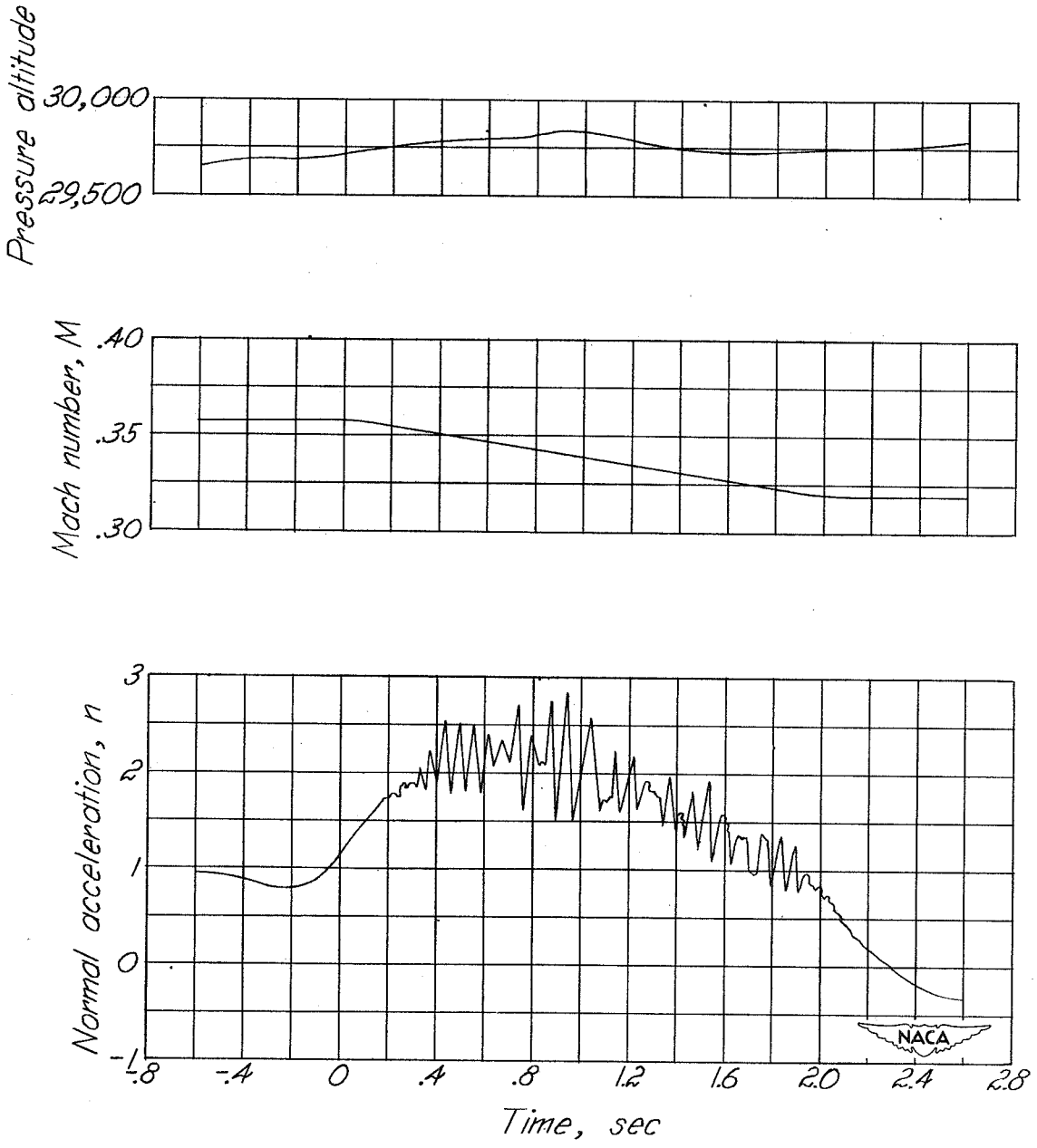

Figure 12.- Time history during a pull-up into a stall at a Mach number of 0.355.

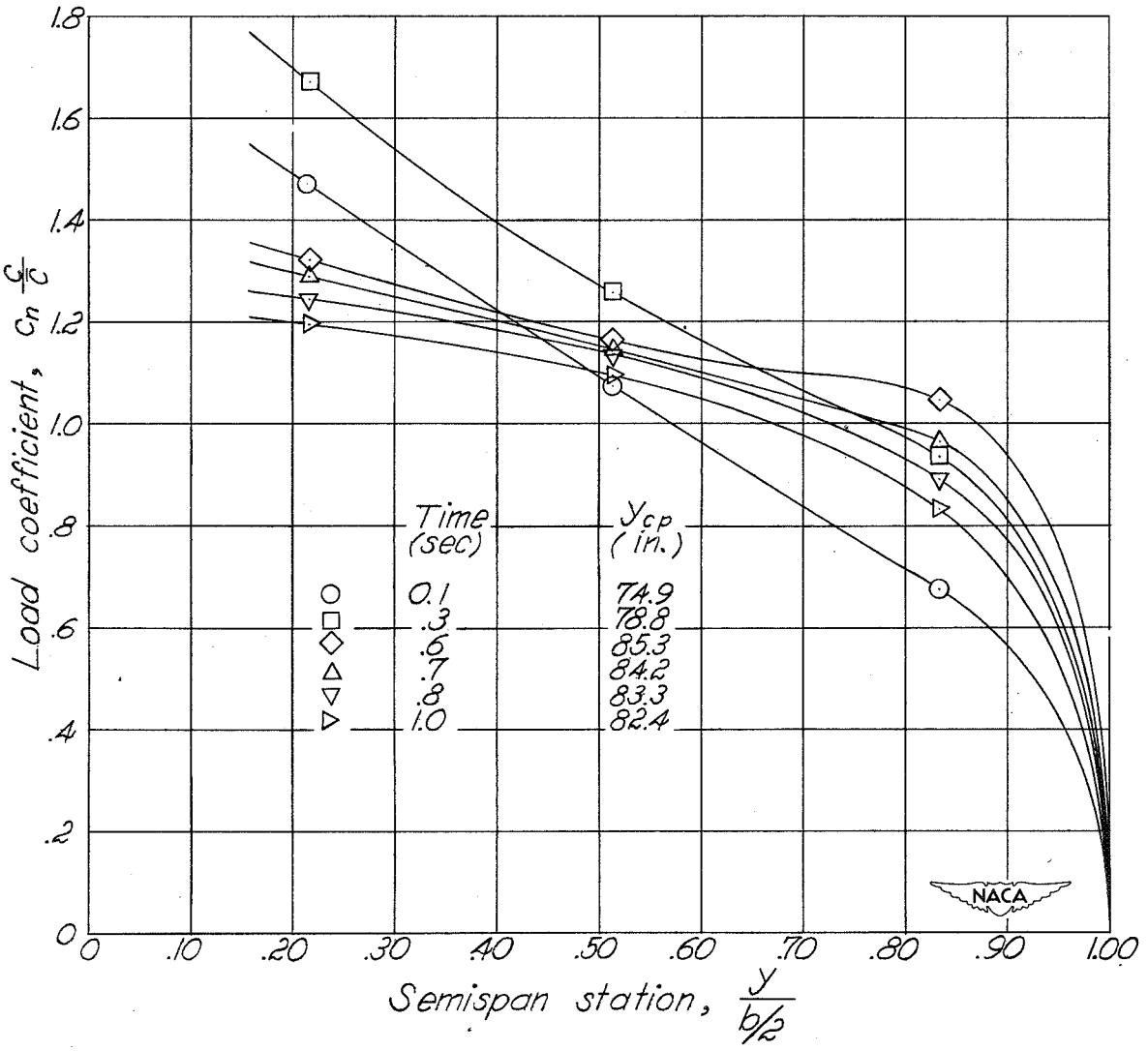

Figure 13.- Left-wing spanwise load distributions for several values of wing normal-force coefficient during a pull-up into a stall at a Mach number of 0.355.

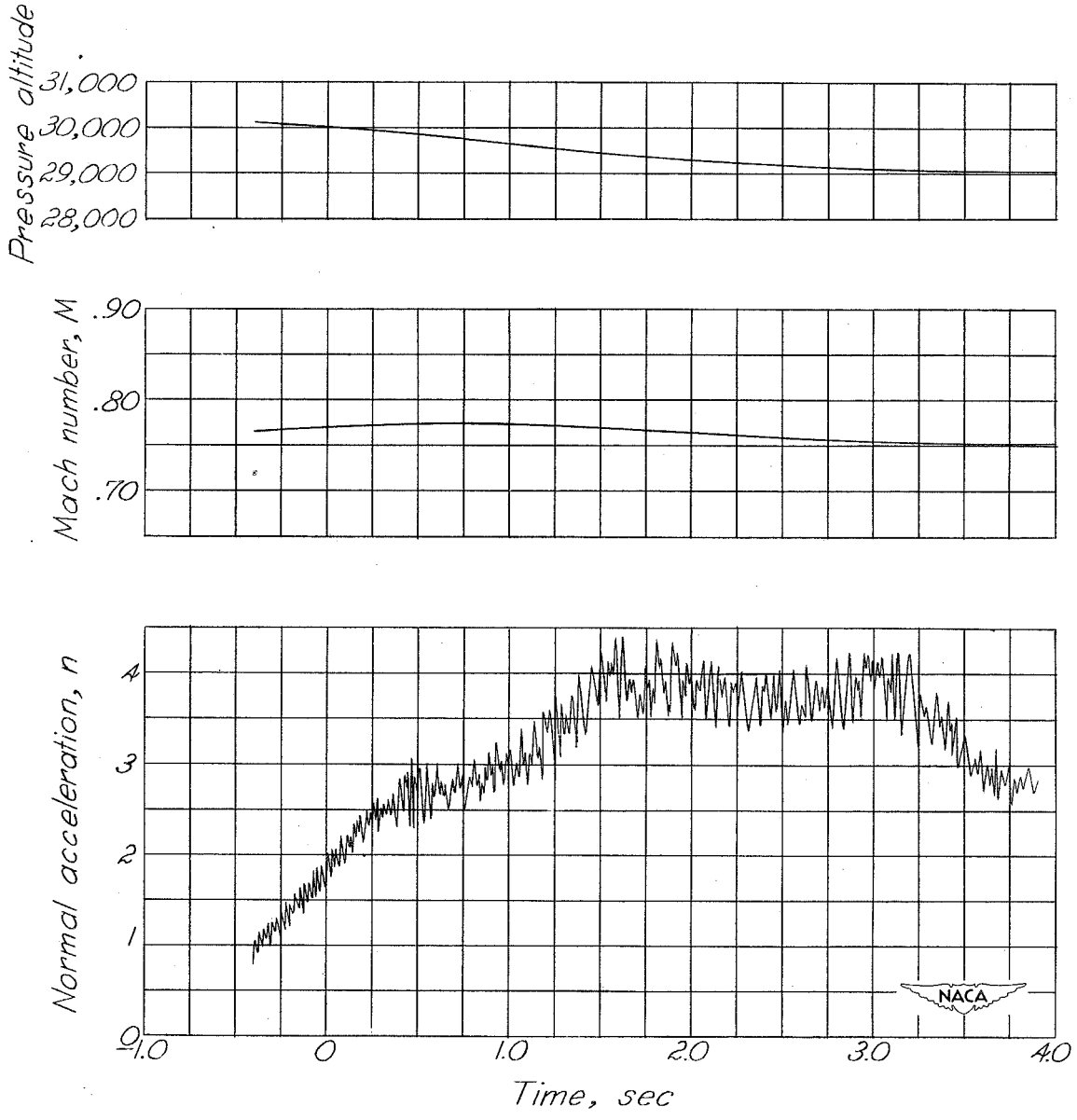

Figure 14.- Time history during a pull-up into the buffeting region at a Mach number of 0.770.

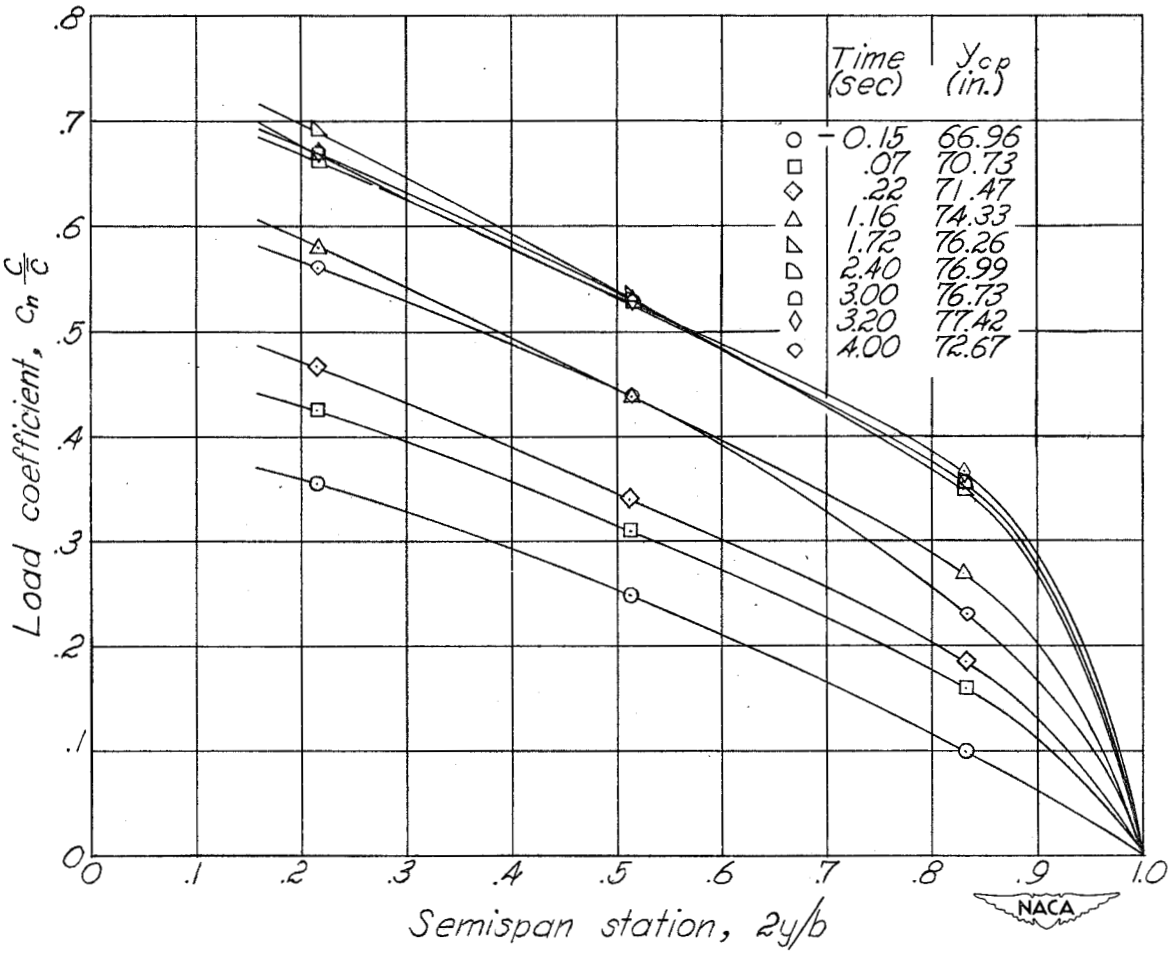

Figure 15.– Spanwise load distributions for several values of wing normal-force coefficient during a pull-up into the buffeting region at a Mach number of 0.770.